Separation Control of a Generic Airfoil using Longitudinal Ridges

Tufan K. Guha, Erik Fernandez and Rajan Kumar
Department of Mechanical Engineering, Florida Center for Advanced Aero-Propulsion
Florida State University, Tallahassee, FL – 32310

ABSTRACT

An experimental investigation was carried out with an objective to enhance the flight envelop of a generic USA-35B wing at low speeds. The technique employed in this study is a pair of longitudinal ridges to take advantage of both leading edge protrusions and chordwise fences. Two-component particle image velocimetry (PIV) was used to measure the velocity field. In the present study, the ridge height and inter-ridge spacing were varied to obtain an optimal control configuration for maximum effectiveness in terms of flow separation region and attachment location. The results showed that the baseline airfoil exhibited a massive flow separation on the suction side at an angle of incidence of 12° and beyond. With the addition of optimal longitudinal ridges, the stall was significantly delayed and the flow was completely attached on the entire airfoil surface up to an angle of incidence of 16°. The study suggest that longitudinal ridges are simple in design, implementation and very effective for separation control.

1. INTRODUCTION

Efforts towards improving the aerodynamic efficiency of various components of an aircraft, particularly the wing, has always been and will continue to be a very active field of interest for aircraft manufacturing companies and the aerospace community at large. The goal in previous studies has been to develop techniques or devices that can enhance the flight envelop, and should be capable of retrofit and easy integration to an existing fleet of aircraft. Flow separation over airfoils, such as those on unmanned air vehicles (UAVs), can lead to an increase in drag and a reduction in lift that may lead to aerodynamic stall and loss of control. The device discussed in this study is a pair of longitudinal ridges, attached on the wing surface to mitigate flow separation at high angles of incidence, delay stall and enhance its aerodynamic efficiency.

Flow over an airfoil separates at high angles of attack due to unfavorable pressure gradients and results in lift loss and drag increment. Depending upon the airfoil thickness, flow separation process can either start from the leading edge of the airfoil or the trailing edge, as the angle of attack is gradually increased. The wing section examined in this study (USA-35B), typically used for remote controlled (RC) aircraft with a potential of UAV applications, is relatively thin and exhibits a leading edge separation. A previous study involving both laboratory experiments and flight tests [1] using this airfoil has shown that the stall occurred at about an angle of attack (α) of 12°. Longitudinal ridges used in the present study push that limit to 16° and beyond. The following sections will discuss pertinent research in the past that has encouraged this present investigation.

Generation of streamwise vortices which energize the boundary layer by increasing momentum mixing near the wall is one of the most effective ways to inhibit separation [2]. Over the years, several devices have been developed which exploit this technique, riblets and vortex generators are the ones that have been extensively investigated among these. Riblets [3] are the symmetrical micro-grooves/wavy structures attached on the surface and aligned along the freestream direction. Studies have shown a skin friction drag reduction of up to 10% on a variety of airfoils with zero or mild pressure gradients at subsonic speeds. Vortex generators are typically vanes that are attached on the wing surface at different streamwise locations and orientations and have proved to be very effective in delaying stall [4]. Longitudinal wing fences [5–6] have been typically used on swept back wing aircraft to enhance aerodynamic performance and improve stall characteristics. Wing fences are typically sharp edge flat plate of height 2–3 times the maximum boundary layer thickness. Williams et al. [6] have

shown that longitudinal fences installed on a T-38 jet trainer aircraft increased its lift coefficient (C_{Lmax}) by 7% and a delay in the attainment of C_{Lmax} by 2°. Their results show that the fences have bound the flow and reduced spanwise movement in addition to a delayed flow separation.

It is interesting to note that such devices are found in nature too and have inspired novel research in the field of bio inspired flow control techniques [7–8]. Humpback whales, which are known to exhibit very high maneuverability, have large scale protuberances called tubercles at the leading edge of their flippers. Fish and battle [8] stated that the flipper cross-section has a similar profile to the NACA 634–021 airfoil. The height of the tubercles range between 2.5% to 12% and the breadth between 10% to 50% of the chord depending on spanwise location. Miklosovic et al. [9] experimentally analyzed a scaled model of a humpback whale flipper in a wind tunnel. They found that the addition of tubercles over the baseline flipper delayed the stall angle by 40% and increased the lift by 6% leading to higher lift/drag ratios. Paterson et al. [10] conducted an unsteady RANS simulation on a NACA 63-021 airfoil with and without equally spaced tubercles. They reported that the tubercles generated chordwise vortices in the troughs between the tubercles, which convect downstream and help in re-energizing the boundary layer. The spanwise distribution of the vortex consisted of a pair of counter-rotating vortices on each side of the individual tubercle's crest. Some of the most recent experimental studies conducted by Hansen et al. [11–13], reported that the spacing between the vortices determine the extent of mixing in the boundary layer, whereas the amplitude/wavelength ratio determines the strength of the vortex.

Yoon et al. [14] numerically investigated wavy leading edge wings, where they kept the amplitude and the frequency of the wave geometry constant but varied the portion of the wing span that was wavy and kept the rest unmodified. They found that at angles of attack beyond the stall angle, the highly modified wing section generated more lift than the baseline. They also clearly showed that the waviness, locally altered the pressure distributions rendering it to be lower in the troughs than the crests. Hence, the pressure gradient behind the trough was more adverse than the crest, forcing the streamlines to bend away from the crests into the troughs. Johari et al. [15] experimentally studied the effect of varying the amplitude and the frequency of the leading edge waviness. They used a NACA 634–021 as their baseline airfoil, the amplitude of the wave ranged between 2.5% to 12% and the frequency between 25% to 50% of the mean chord length. They observed that variation in amplitude had a distinct effect on the aerodynamic performance while the variation in frequency had none. At angles below the baseline stall angle, the modified airfoil showed detrimental results, like reduced lift and increased drag, but beyond the stall angle, the lift recovered and was 50% higher than the baseline airfoil with negligible drag penalty.

An extension to a wavy leading edge is a wing with a wavy surface, experimentally studied by Zverkov et al. [16]. They noted that the leading edge separation bubble present on the baseline airfoil at higher angle of attack was broken into small pockets of separation in the troughs of the wavy surface. The authors also presented a detailed discussion on boundary layer transition and associated instabilities. They concluded that on the hump of the wavy surface, unlike the troughs, the transition from a laminar to turbulent boundary layer took place without any flow separation or excitation of instability modes.

In the present study, we have exploited the benefit of both leading edge devices and chordwise vortices by introducing longitudinal ridges. For the present experimental investigation, longitudinal ridges were made of circular, flexible plastic tubes which can be attached longitudinally (chordwise) on the surface of the airfoil. They were covered with thin tape to render a smooth profile. The radius of the tube and their intermediate separation distance were the two geometric parameters that were varied and compared to find the most effective combination. Quantitative velocity field measurements at the mid-span plane, between the two ridges were acquired with the help of 2D-Particle Image Velocimetry (PIV). The ridges were found to be effective at all the test conditions and the optimized configuration delayed stall by more than 30% of the baseline.

2. EXPERIMENTAL SETUP

2.1. Test Model

The wing-section under examination was a USA-35B profile, which is similar to the NACA-4412. The same wing-section had been previously used to study the effect of microjets on flow control [1, 17] and was found receptive to flow control techniques. It had a span of 610 mm, so it flushed with the walls of the test section and a chord length of 370 mm, as shown in Figure 1. The airfoil was mounted at a distance of 203 mm (0.55 C) downstream of the beginning of the test-section and 304 mm (0.82 C)

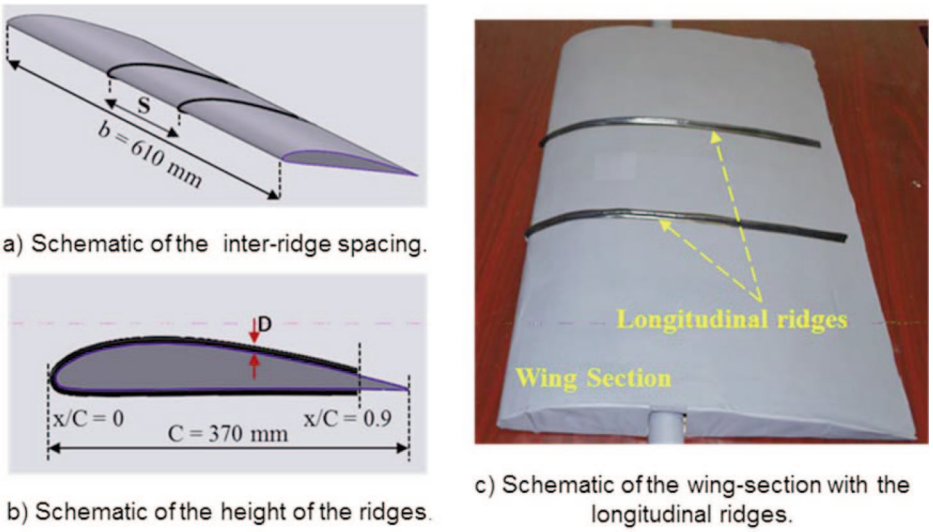

Figure 1. Schematics and picture of the wing section with longitudinal ridges.

from the floor of the wind tunnel. The wing could be rotated and fixed at any particular angle of attack between –4° to 20°. The incoming boundary layer thickness (δ) at quarter-chord measured with a pitot tube was approximately 4 mm and the corresponding non-dimensionalized δ/C was equal to 0.01.

The modified wing had two longitudinal ridges going over its surface, parallel to each other, at equal distance from the mid-span plane. The ridges covered upto 90% of the chord length on both the suction and the pressure sides, so as not to affect the sharp trailing edge of the wing. Longitudinal ridges were made from circular flexible plastic tubes. The diameter and the inter-ridge spacing were the two variable parameters in these experiments and ranged between 1.27 mm to 5.08 mm and 25.4 mm to 203.2 mm, respectively. The height of the ridges were non-dimensionalized with the measured boundary layer thickness at quarter chord and the inter-ridge spacing with the chord length and tabulated in Table 1, representing the full set of experimental test conditions. It should be noted that the heights of the ridges were of the order of the boundary layer thickness at quarter chord location.

2.2. Low Speed Wind Tunnel Facility

Measurements were made in the low speed wind tunnel (Figure 2) at the Florida Center for Advanced Aero-propulsion (FCAAP) at the Florida State University. Wind tunnel velocity was measured by a pitot-static probe mounted 200 mm upstream of the test section. The test section had dimensions of 610 mm × 610 mm × 1524 mm and was manufactured with acrylic walls, which allowed for flow visualization from all four sides. Accurate velocities could be obtained between a range of 9–90 m/s with a test section freestream turbulence intensity ≤ 0.5% at 20 m/sec. The present tests were carried out at a freestream velocity of 20 m/sec and at a corresponding Reynolds number of 5.1×10^5 based on a chord length of 370 mm.

2.3. Particle Image Velocimetry (PIV) Measurements

Two-dimensional planar particle image velocimetry (PIV) was used to obtain quantitative measurements of the flow field of interest. For all planar PIV cases presented, measurements were

Table 1. Experimental test conditions

Parameter	Symbol (Dimension)	Parametric values
Angle of attack	α (°)	0, 12, 14, 16
Height of ridge	D (mm)	1.27, 2.54, 5.08
		(0.05, 0.1, 0.2 inches)
Non-dimensionalized	*D/δ*	*0.3, 0.6, 1.3*
Inter-ridge spacing	S (mm)	25.4, 50.8, 101.6, 152.4, 203.2
		(1, 2, 4, 6, 8 inches)
Non-dimensionalized	*S/C*	*0.07, 0.14, 0.28, 0.42, 0.56*

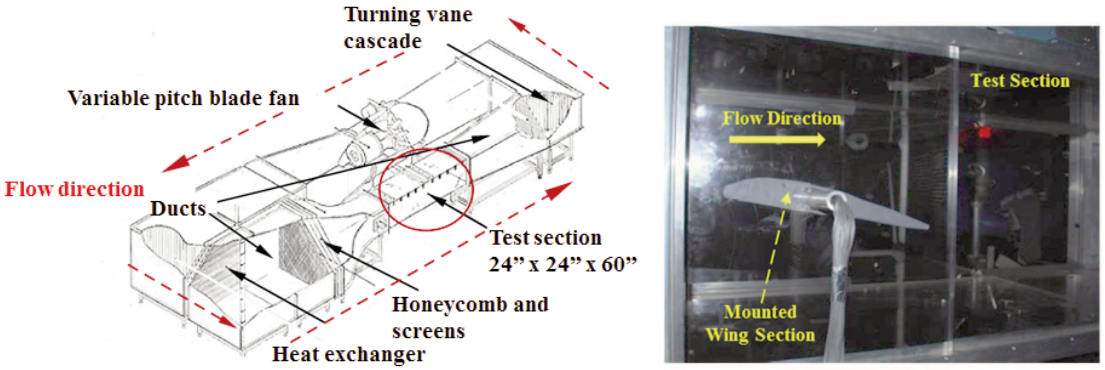

a) Sketch of the closed loop, low speed wind-tunnel. b) Airfoil mounted in the test section.

Figure 2. Experimental Setup, showing the sketch of the subsonic wind tunnel and a picture of the airfoil in the test section.

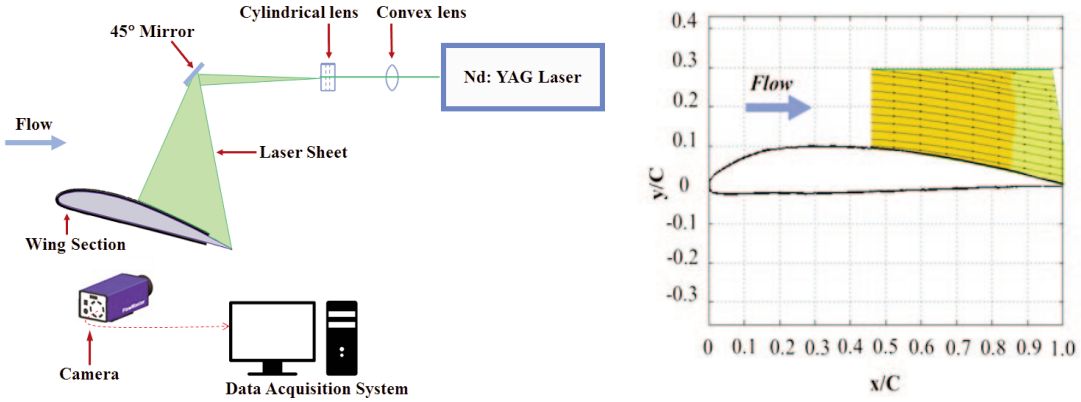

Figure 3. Two dimensional-PIV setup and measurement location on the airfoil.

carried out at the airfoil mid-span (x-y plane) and the flow was examined over the aft ~ 60% of the airfoil to capture the separation effects. Figure 3 shows the PIV setup, measurement location and the extent of the laser sheet on the airfoil, mostly covering the region of interest in terms of flow separation and attachment locations. The measurement region with respect to airfoil slightly varied with angle of attack, as laser sheet position was fixed. The flow was illuminated by a pulsed Quantel® Nd: YAG laser triggered at a specified time interval. The beam was focused using a single spherical lens of 1m focal length and the laser sheet was created when the beam passed through a cylindrical lens. The air flow was seeded using a ROSCO® fog machine and introduced into the wind tunnel upstream of the flow straighteners. The seed particles were approximately 2–3 μm in size. The time interval between the laser pulses was approximately 30 μs for the presented cases. Image pairs were acquired at 15 Hz with a resolution of 2560 × 2160 pixels. A mean of 500 and 1000 instantaneous ensemble image pairs were used for finding the steady and the unsteady flow parameters, respectively. Images were acquired and processed using LaVision Davis 8 software with a 5.5 megapixel sCMOS camera equipped with a 55 mm focal length lens. Image correlations were made using a final adaptive interrogation window size of 48 × 48 pixels with a decreasing size multipass algorithm. All passes used a 50% window overlap. The measurement uncertainty was estimated to be about 1% in ensemble-averaged and 5% in rms velocity measurements with a 95% confidence level, respectively.

3. RESULTS AND DISCUSSION

The main objective of the present study is to experimentally examine the effect of longitudinal ridges to control flow separation on the suction surface of the airfoil at approach-to-stall conditions and study the effect of geometrical parameters on its performance.

3.1. Baseline Flow

Figure 4 shows the effect of angle of attack on the time-averaged streamwise velocity contours for the baseline airfoil. The results are shown in terms of normalized streamwise velocity (U/U_{in}, where U_{in} is the incoming freestream velocity) and streamwise velocity fluctuations (U_{rms}/U_{in}). The arrowheads in the streamlines indicate the direction of flow. As expected, the flow is completely attached at $\alpha = 0°$ (Figure 4a), decelerates on the aft end, and the surface streamlines follow the contour of the airfoil. With an increase in the angle of incidence to $\alpha = 12°$ (Figure 4b), the flow separates on the airfoil suction side approximately at $x/C = 0.65$ and a separation region is formed with open separation (no indication of attachment at the trailing edge). With further increase in angle of incidence to 14° (Figure 4c), the size of the separation region (blue region) is significantly increased and the separation location is moved upstream ($x/C < 0.5$) leading to massive stall, indicated by reverse flow near the airfoil surface. The separating streamline is nearly parallel to the freestream.

The streamwise velocity fluctuations and velocity profiles extracted at three streamwise locations from Figure 4c are shown in Figure 5. The inflection point (marked as "A") in the velocity profile (Figure 5b) marks the boundary of the growing separation region and indicates the position of the separated shear layer. The growing separation region causes the separated shear layer to move away from the airfoil surface, represented by the receding green band of large velocity fluctuations observed in Figure 5a. The turbulent shear layer involving high velocity fluctuations in the streamwise direction

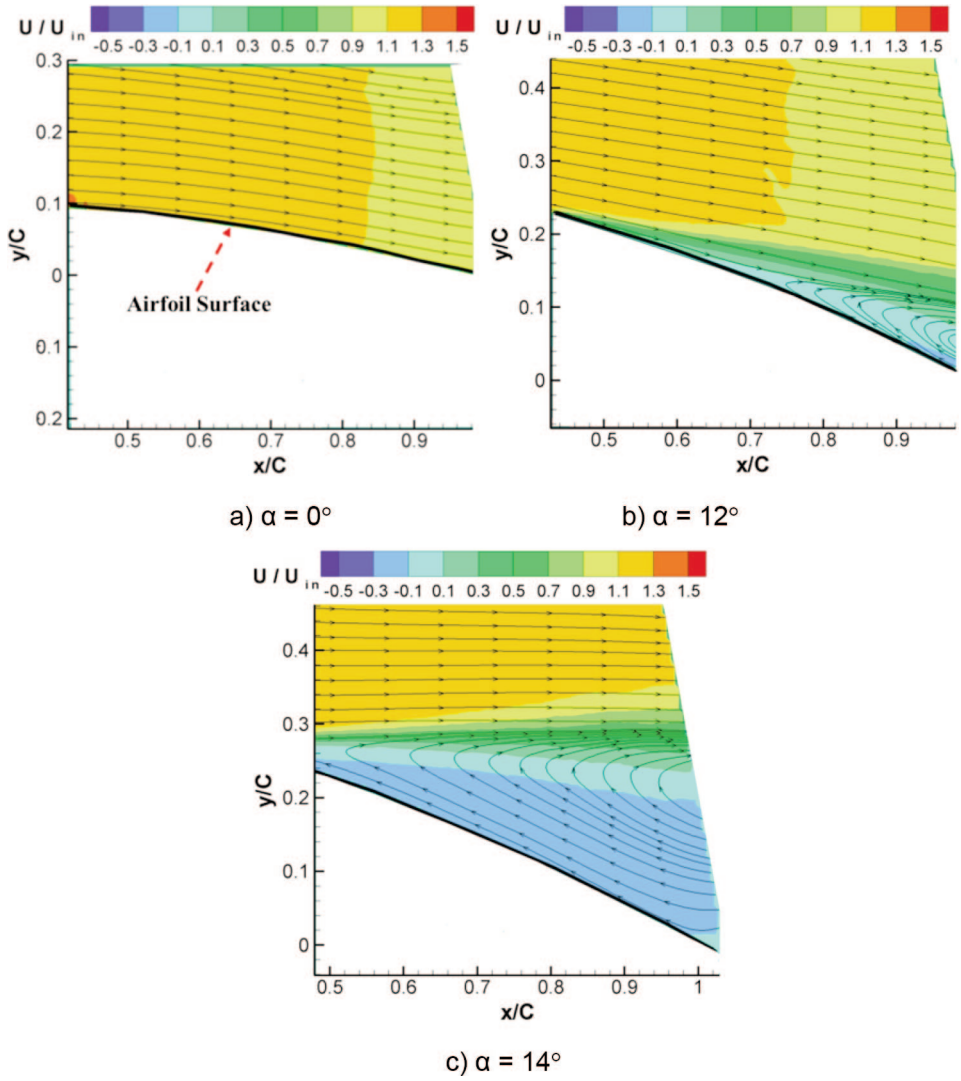

Figure 4. Time-averaged streamwise velocity contours for the baseline airfoil at different angles of attack.

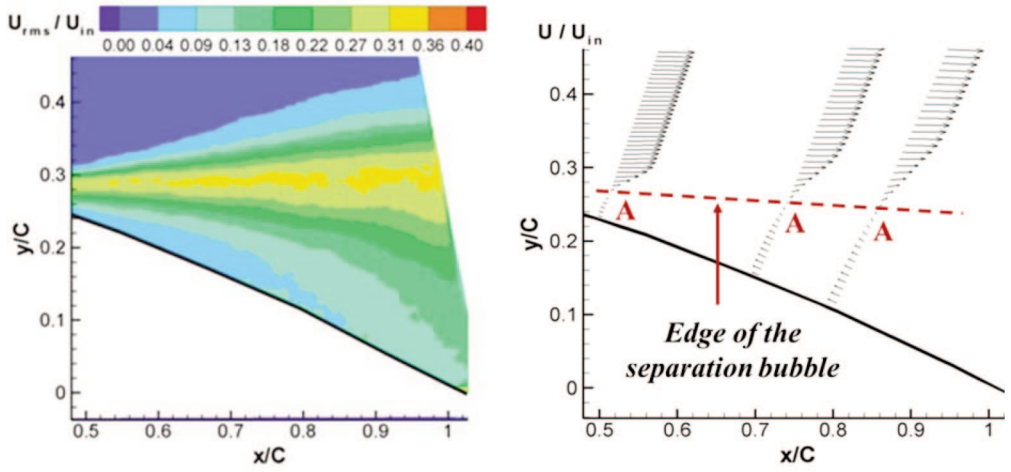

a) Streamwise Velocity Fluctuations b) Velocity Profiles

Figure 5. Streamwise velocity fluctuations and velocity profiles for baseline airfoil at $\alpha = 14°$.

(Figure 5a) is separated and seems to diverge away from the airfoil surface once again indicating an open separation causing massive stall.

3.2. Airfoil with Longitudinal Ridges

Two chordwise longitudinal ridges were placed on the airfoil near the mid-section on either side of the airfoil centerline (Figure 1c). The height of the ridges and their inter-spacing were the two parameters varied and their effects have been presented in the following sections.

3.2.1. Effect of ridge height

Figure 6 shows the effect of various ridge heights tested, in affecting the flow separation on the airfoil, for a fixed inter-ridge spacing of S/C = 0.14, at an angle of incidence of 14°. The dotted line indicates the airfoil surface and the solid line represent the outer edge of the chordwise ridges (Figure 6a). In comparison to the boundary layer thickness estimated at quarter-chord ($\delta = 4$ mm), the two sets of small thickness ridges (0.3 δ and 0.6 δ) were well within the boundary layer whereas a ridge height of 1.3 δ was slightly outside. The height of the ridges was restricted to the order of the boundary layer, so as not to cause a significant increase in the parasitic drag.

The results clearly show that in comparison to baseline flow at $\alpha = 14°$ (Figure 4c), even a pair of very thin ridges (0.6 δ) (Figure 6a), reduces the size of separation region considerably and pushes the separation location downstream (~x/C = 0.7). With an increase in ridge height to 1.3 δ (Figure 6b), the flow is completely attached over most of the airfoil surface. In comparison to baseline configuration (Figure 5a), the turbulent shear layer is moved much closer to the airfoil surface and its associated high velocity fluctuations are significantly reduced with control, as shown in Figures 6c and 6d. This mixing layer brings in momentum from the freestream mean flow and helps to energize the flow close to the surface, enabling it to counteract the decelerating effect of the severe adverse pressure gradient on the aft end of airfoil at high angles of incidence.

An important point to be noted is that though this arrangement of ridges was able to push separation location significantly downstream, the velocities close to the surface were still very low (Figures 6e and 6f) and any small increase in angle of attack may result in flow separation. The flow near the surface is attached but not very energetic and therefore prone to separation. Thicker ridges appear to be more effective in restraining the shear layer. This situation was further improved upon when the inter-ridge separation was increased to higher values, discussed in the following section. The thinnest ridges ($D/\delta = 0.3$) showed negligible control effectiveness, therefore the results are not presented or discussed.

3.2.2. Effect of spacing between the ridges

The effect of inter-ridge spacing on the streamwise velocity at an angle of attack of 14° is shown in Figure 7. In comparison to the baseline flow (Figure 4c), when the ridges were placed relatively close

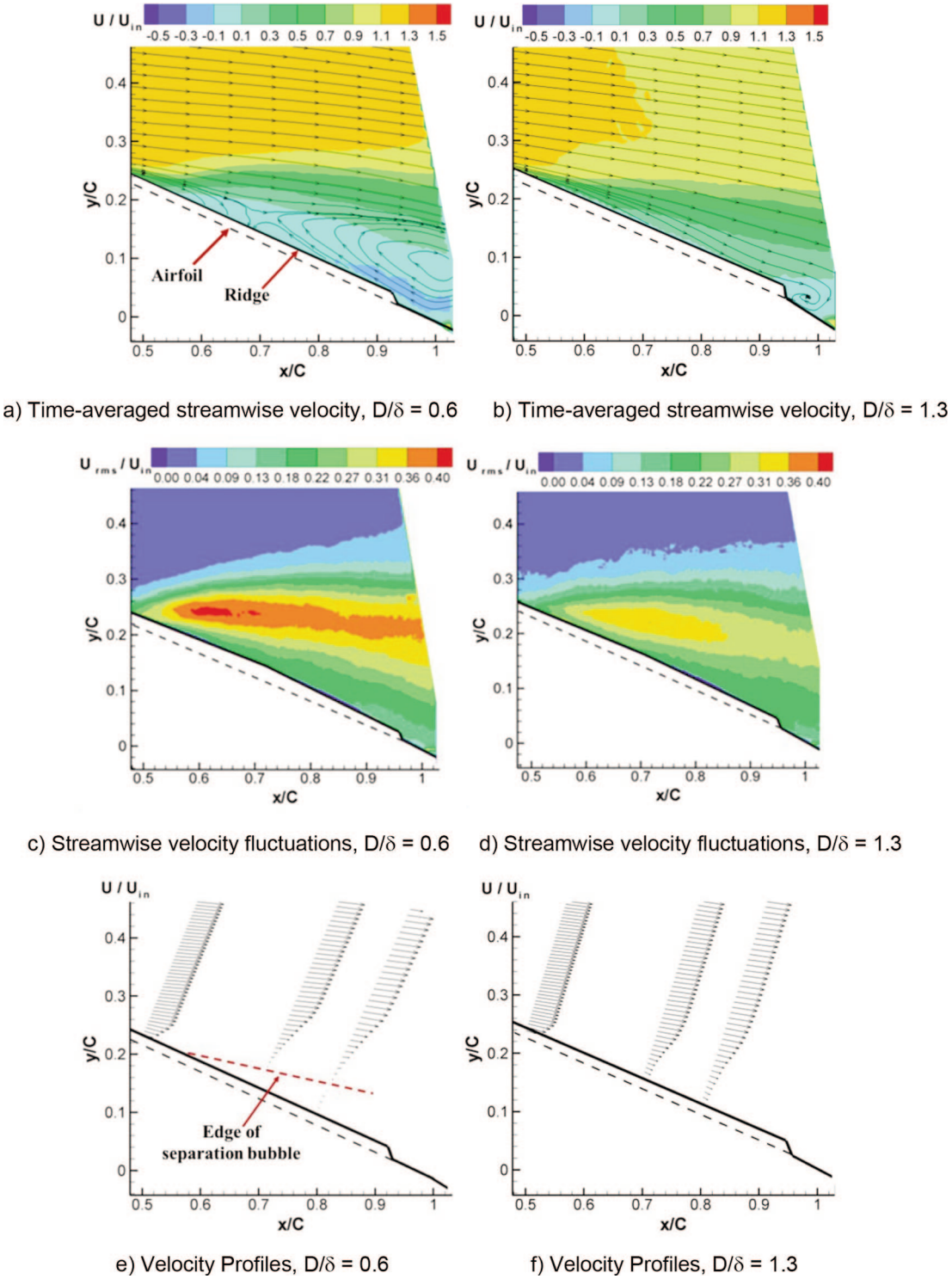

Figure 6. Effect of ridge height on velocity distributions for a fixed inter-ridge spacing of S/C = 0.14 at α = 14°.

to each other, S/C = 0.07 (Figure 7a), the effectiveness in terms of delay in separation location, or the size of the separation region was minimal, if any. However, as the spacing between the two ridges was initially increased to 0.14 C and then 0.28 C (Figures 7b and 7c), its effectiveness improved and the separated flow region was nearly eliminated on the entire surface. These results suggest that the mechanisms responsible for flow reattachment to be effective require sufficient spacing between the two ridges. The effectiveness was further improved with an increase in spacing to 0.42 C (Figure 7d) in terms of reduction in the

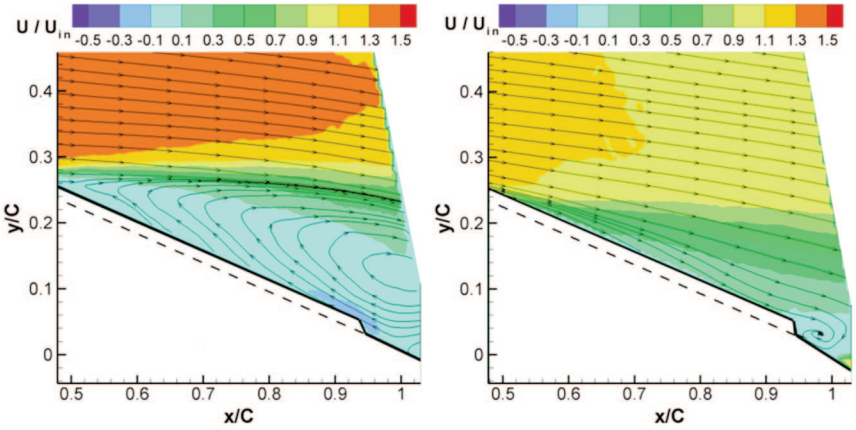

a) Time-averaged streamwise velocity, S/C = 0.07 b) Time-averaged streamwise velocity, S/C = 0.14

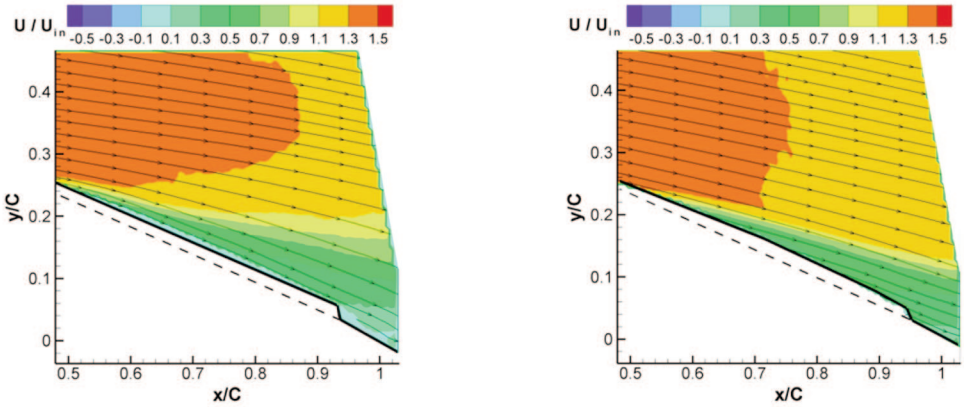

c) Time-averaged streamwise velocity, S/C = 0.28 d) Time-averaged streamwise velocity, S/C = 0.42

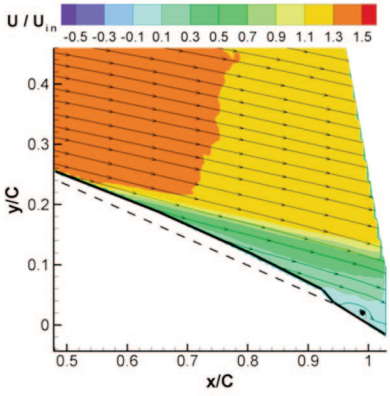

e) Time-averaged streamwise velocity, S/C = 0.56

Figure 7. Effect of ridge spacing on time-averaged streamwise velocity distributions at a fixed ridge height of D/δ = 1.3 at α = 14°.

thickness of shear layer and bending of streamlines towards the airfoil surface. However, when the spacing was further increased to 0.56 C (Figure 7e), formation of a small separation region was observed near the trailing edge of the airfoil. This may be due to the fact that for S/C = 0.56, measurement location (airfoil mid plane) is far from the control i.e. longitudinal ridges.

In comparison to the baseline airfoil, the streamwise velocity fluctuations for the modified airfoil with the optimum ridge height (1.3 δ) and inter-ridge spacing of 0.42 C show a significant modification

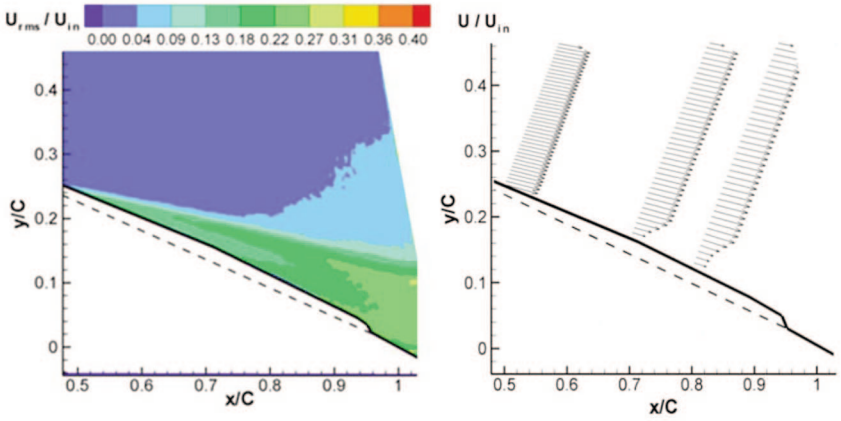

a) Streamwise velocity Fluctuations, D/δ = 1.3, S/C = 0.42 b) Velocity Profiles, D/δ = 1.3, S/C = 0.42

Figure 8. Non-dimensional Urms contour and velocity profile at α = 14°, D/δ = 1.3 and S/C = 0.42.

in the shear layer development and improvement in the flow characteristics. The turbulent shear layer that was completely separated and diverging for the baseline case (Figure 5a), is now completely reattached to the surface (Figure 8a) and is significantly thinner. The velocity profiles for the airfoil with ridges (Figure 8b) show positive velocity vectors on the entire surface and the velocity magnitude is reasonably high even very close to the airfoil surface. These results clearly suggest that the airfoil with longitudinal ridges will produce significantly lower drag even at an angle of incidence of 14°, for which the baseline airfoil was completely stalled.

3.2.3. Control effectiveness at higher angles of attack

As discussed in the previous sections, the flow was separated on the suction side and the baseline airfoil was stalled at an angle of incidence of 12°. With the application of control (longitudinal ridges) the flow was completely attached up to an angle of incidence of 14°. In order to extend the flight envelop, the angle of incidence was further increased to 16° with the optimal control configuration. A comparison between flow characteristics of the baseline airfoil and the airfoil with the optimum longitudinal ridges (1.3 δ, 0.42 C) is shown in Figure 9. As expected, the baseline airfoil shows (Figures 9a and 9c) a large open separation with very high negative velocities near the wall leading to a massive stall. The turbulent shear layer is thick, separated and diverging away from the airfoil surface. The velocity vectors are pointing away from the surface (Figure 9e) and the vertical distance of the inflection point from the airfoil surface increases moving downstream.

With the application of control (Figures 9b, 9d and 9f), the separation on the airfoil surface is completely eliminated and the flow is restrained effectively even at α = 16°. The turbulent shear layer is much thinner and attached. The velocities near the wall are about 50% of the freestream magnitude and vectors pointing along the surface. These results clearly show that the control technique employed here has delayed the stall angle for this airfoil up to 16° and beyond. The present study has clearly demonstrated the use of a pair of longitudinal ridges as an effective means of flow separation control on USA-35B airfoil at approach-to-stall conditions.

4. CONCLUSIONS

An experimental investigation to demonstrate the effectiveness of a pair of longitudinal ridges on the aerodynamic characteristics of a USA-35B airfoil, at a Reynolds Number of 5.1×10^5, has been carried out at FSU low speed wind tunnel. Particle image velocimetry was used to study the streamwise velocity field and measure the flow control effectiveness in terms of delay in flow separation on the suction side of airfoil. The height and the inter-spacing between the ridges were the two parameters that were varied in these experiments. The results showed that two chordwise ridges of optimal height (of the order of the boundary layer) and inter-ridge spacing completely eliminated the flow separation and accelerated the flow on the suction side of this airfoil. Incorporation of the longitudinal ridges resulted in a delay in its stall angle up to 16°. The present experimental study, a proof-of-concept, has demonstrated the effect of a geometrically simple flow control technique that can be easily

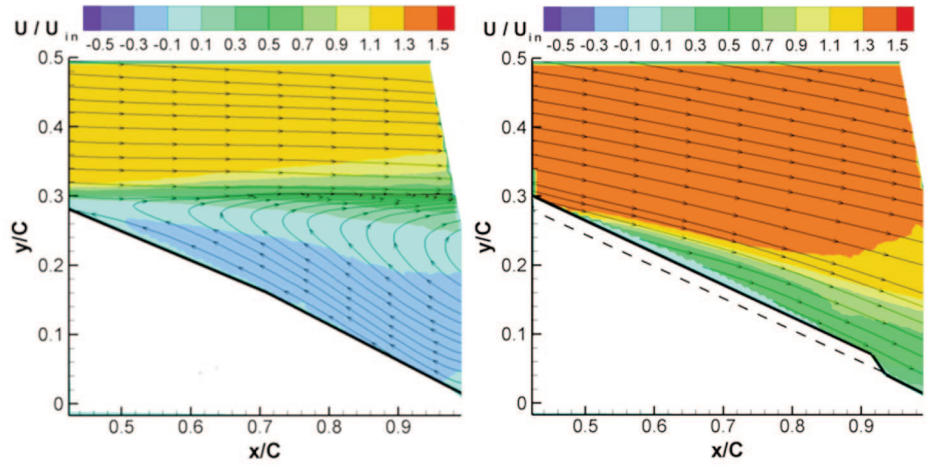

a) Time-averaged streamwise velocity, baseline airfoil b) Time-averaged streamwise velocity, D/δ = 1.3, S/C = 0.42

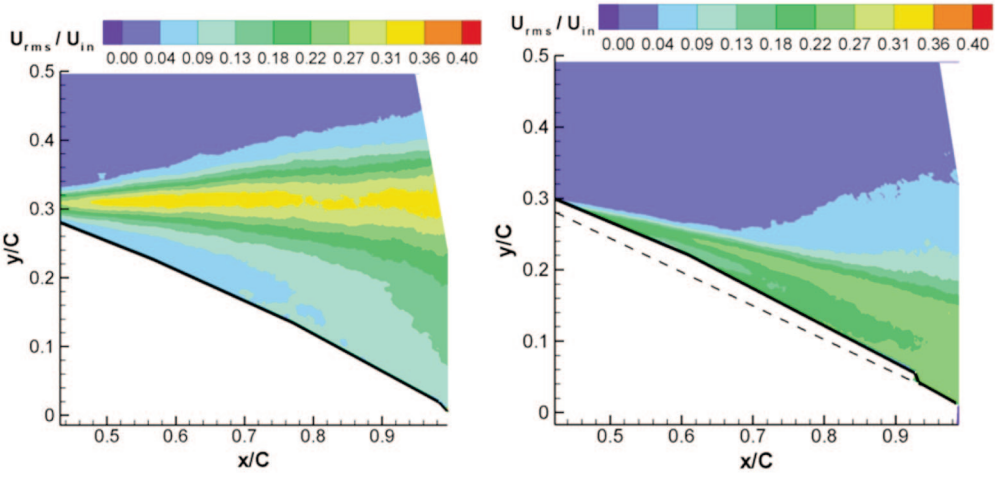

c) Streamwise velocity fluctuations, baseline airfoil d) Streamwise velocity fluctuations, D/δ = 1.3, S/C = 0.42

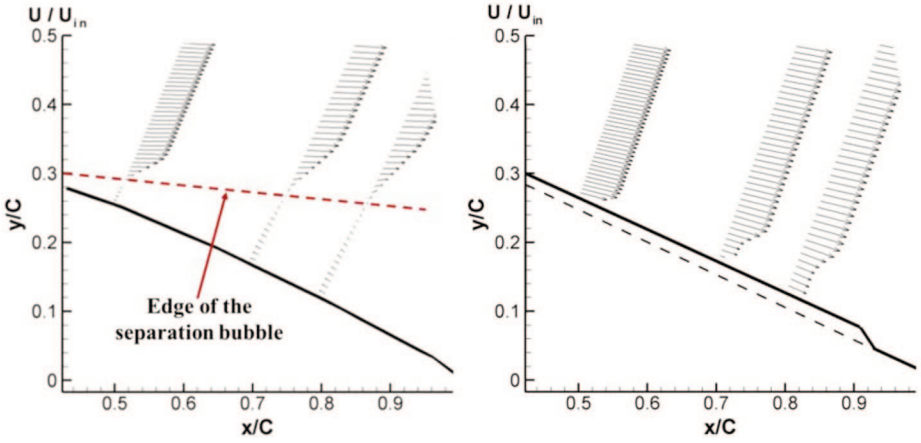

e) Streamwise Velocity Profiles, baseline airfoil f) Streamwise Velocity Profiles, D/δ = 1.3, S/C = 0.42

Figure 9. Streamwise Velocity Characteristics at α = 16°.

implemented in enhancing the flight envelop of a UAV. Future work would include multiple ridge pairs of optimal geometry encompassing the entire span of the wing section and measurement of aerodynamic forces and moments using a strain gage balance.

REFERENCES

[1] Kreth, P. and Alvi, F., Microjet-based active flow control on a fixed wing UAV, *Journal of Flow Control, Measurements & Visualization*, 2014, 2, 32–41.

[2] Gad-el-Hak, M. and Bushnell, D. M., Separation control: review, *Journal of Fluids Engineering*, 1991, 113(1), 5–30.

[3] Viswanath, P. R., Riblets on airfoils and wings-A review, *AIAA Paper* 1999, 99–3402.

[4] Lin, J. C., Review of research on low-profile vortex generators to control boundary-layer separation, *Progress in Aerospace Sciences*, 2002, 38(4), 389–420.

[5] Rossow, V., Two-fence concept for efficient trapping of vortices on airfoils, *Journal of Aircraft*, 1992, 29(5), 847–855.

[6] Williams, M. D., Reeder, M. F., Maple, R. C. and Solfelt, D. A., Modeling, simulation and flight tests for a T-38 Talon with wing fences, *Journal of Aircraft*, 2010, 47(2), 423–433.

[7] Watts, P. and Fish, F. E., The Influence of Passive, Leading Edge Tubercles on Wing Performance, in: *Proceedings of the Twelfth international symposium on unmanned untethered submersible technology*, 2001, Autonomous Undersea Systems Institute, Durham, New Hampshire, 1–5.

[8] Fish, F. E. and Battle, J. M., Hydrodynamic Design of the Humpback Whale Flipper, *Journal of Morphology*, July 1995, 225, 51–60.

[9] Miklosovic, D. S., Murray, M. M., Howle L. E. and Fish F, E., Leading-Edge Tubercles Delay Stall on Humpback Whale (Megaptera Novaeangliae) Flippers. *Physics of Fluids (1994-present)*, 2004, 16(5), 39–42.

[10] Paterson, E. G., Wilson R. V. and Stern F., General Purpose Parallel Unsteady RANS CFD Code for Ship Hydrodynamics, *IIHR Hydrosci, Eng. Rep.*, 2003. 531.

[11] Hansen, K. L., Kelso, R. M. and Dally, B. B., The Effect of Leading Edge Tubercle Geometry on the Performance of Different Airfoils, in: *World*, 2009, Krakow, Poland.

[12] Hansen, K., *Effect of leading edge tubercles on airfoil performance*, Ph.D. Thesis, School of Mechanical Eng., Adelaide University, Australia, 2012.

[13] Hansen, K. L., Kelso, R. M. and Doolan, C. J., Reduction of Flow Induced Tonal Noise Through Leading Edge Tubercle Modifications, in: 16th AIAA/CEAS Aeroacoustics Conference, AIAA Paper 2010-3700, June 7–9, 2010, Stockholm, Sweden.

[14] Yoon, H.S., Hung, P.A., Jung, J.H. and Kim, M.C., Effect of Wavy Leading Edge on Hydrodynamic Characteristics for flow Around low Aspect Ratio Wing, *Computers & Fluids*, 2011, 49(1), 276–289.

[15] Johari, H., Henoch, C., Custodio, D. and Levshin, A., Effects of Leading-edge Protuberances on Airfoil Performance, *AIAA Journal*, 2007, 45(11), 2634–2642.

[16] Zverkov, I., Zanin, B. and Kozlov, V., Disturbances Growth in Boundary Layers on Classical and Wavy Surface Wings, *AIAA Journal*, 2008, 46(12), 3149–3158.

[17] Kreth, P., Alvi, F., Kumar, V. and Kumar, R., Microjet Based Active Flow Control on a Fixed Wing UAV, in: 48th AIAA-Aerospace Sciences Meeting, AIAA paper 2010-1260, January 4–7, 2010, Orlando, Florida.